Chapter 1

Introduction

The atomic nucleus was discovered in 1911 by Ernest Rutherford. He had demonstrated that the large angle α particle scattering can be explained only in term of a positively charged nucleus. The nucleus is a cluster of protons and neutrons occupying a small region at the center of the atom, it's diameter is of the order of 10^{-14} meter which is about 10^3 times smaller than the diameter of the atom. Since then, nuclear reactions have been extensively used to study the structure of nuclei by investigating the properties like size, shape, lifetimes, transition rates, etc. and finding the interaction potential between the interacting nuclei. In connection to the results obtained from the α scattering experiment, Rutherford had suggested the need for using projectiles with energies higher than those obtained by naturally occurring radioactive substances which he thought would help in probing the nuclear structure further. Nuclear reaction can occurs when atomic particles come together at very close, where feel strong nuclear force [6]. Thus the accelerator facility has opened for the understanding the character of atomic particles at high temperature and angular momentum. Most of the known nuclear reactions are produced by exposing different materials to a beam of accelerated sub atomic particles. Usually density overlap and large energy and momentum exchange takes place and the final products of the reaction are one, two, or more nuclear particles leaving the point of close contact in various directions. The products are mostly of a species different from the particles in the original pair. Fig.1.1 shows the

different type of nuclear reactions, distinguished on the basis of impact parameters.

1.1 Description of a nuclear reactions

Types of nuclear reactions

When a projectile a is bombarded on a target X, different nuclear reactions occur. These process can be broadly classified as (i)Elastic scattering, (ii) Direct reactions and (iii) Compound Nuclear reactions. The latter two are classified according to the interaction time between the colliding nuclei *i.e.* the relaxation time required for various degrees of freedom in the interaction [7].

Consider nuclear reactions of the type.

$$a + X \rightarrow Y + b \tag{1.1}$$

or, in more compact notation, $X(a, b)Y$. The notation means that particle a strikes nucleus X to produce nucleus Y and an outgoing particle b.

1.1.1 Elastic scattering

The projectile and the target before and after the scattering, their ground states is not changed. Elastic scattering can be used to get information on the interaction radii, surface thickness (diffuseness), interaction potential (via the optical model potential calculations), grazing angular momentum, and reaction cross-sections. Kinetic energy is also same before and after scattering in the center of mass system. This is a peripheral collision in terms of impact parameter.

$$a + X \rightarrow X + a \tag{1.2}$$

1.1.2 Inelastic scattering

In this type of reaction, interacting particles remain unchanged before and after scattering but any or both of the interacting particles may be excited through mutual

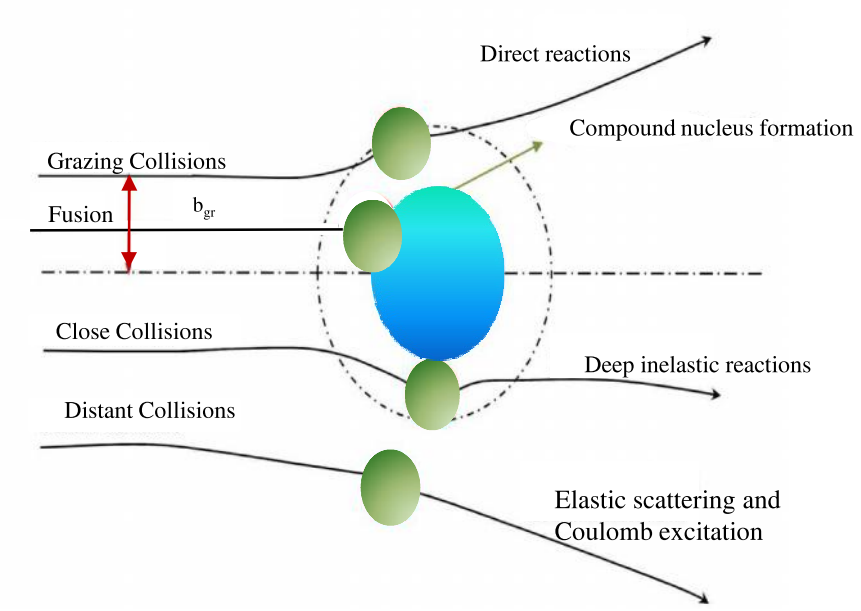

Figure 1.1: Types of reaction processes distinguished on the basis of the impact parameter at which these reactions occur.

excitation process with reduction in initial kinetic energy. such as,

$$a + X \rightarrow X^* + a^* \tag{1.3}$$

The cross section for such inelastic scattering provides information on the nuclear spin and parity of the excited states.

1.1.3 Transfer reactions

In transfer reactions, when the projectile passes over the periphery of the target one or more nucleons are transferred between the projectile and the target. When, projectile gains the nucleons from the target nucleus as it passes from the periphery of the target nucleus. This type of transfer reaction is called "Pick up reaction". When, projectile transfers the nucleons to the target nucleus as it passes from the periphery of the target nucleus. This type of transfer reaction is called "Stripping reaction".

1.1.4 Knock-out reactions

In this kind of reactions, a nucleon or light nucleus get ejected from the target nucleus by the projectile. This will produce three particles in the final state. In this reaction the projectile remains free before knocking the target nucleon or light nucleus, it is also known as quasi-free scattering.

In the direct interaction process two nuclei make just glancing contact. For this reason these types of reactions are also known as peripheral reactions. It is assumed that in this kind of reactions, nuclear particles enters or leave the target nucleus without disturbing other nucleon that are available in the nuclear shell. The time span for these kind of reactions are $\sim 10^{-21}$sec. Direct reactions may proceed from initial to final partition without going through the intermediate state. Direct reactions are very suitable in providing information regarding the relation (overlap) between the ground state of target nucleus and a ground or a particular excited state of a residual nucleus.

1.1.5 Compound nuclear reactions

The compound-nucleus model is a description of atomic nuclei proposed in 1936 by Niels Bohr [8, 9] to explain nuclear reactions as two stage process comprising the formation of relatively long lived intermediate nucleus and its subsequent decay. First a bombarding projectile loses all its energy to the target nucleus and become an integral part of a new, highly excited, unstable nucleus, called *compound nucleus*. The formation stage takes the time approximately equal to the time interval for the bombarding particle to travel across the diameter of the target nucleus [10].

$$\Delta t \sim \frac{R}{c} \sim 10^{-21} s. \tag{1.4}$$

The compound nucleus is highly excited and has a temperature; it is 'hot'. It also caries angular momentum equal to the sum of the angular momentum of the relative motion in the entrance channel and the spins of the initial collision partners. The excitation energy and the angular momentum of the compound nucleus eventually released via a decay into smaller fragments. For compound nucleus at excitation energies corresponding incident laboratory energies E<10 MeV per nucleon of the fused system, the decay can categorized in two main schemes [11, 10].

(i) *Evaporation*, *i.e.* emission of light particle like neutrons, protons, α-particles, and so on. There remains a bound residual nucleus called *evaporation residue* of a slightly lower mass than the compound nucleus. The particle evaporation is generally accompanied by the γ-ray emission, which has to be taken into account in the energy and angular momentum balance.

(ii) *Fission*, where the compound nucleus splits up into two halves of more or less equal size. This process is accompanied by evaporation of light particle out of the fissioning nucleus, similarly the fission fragment will generally decay further by evaporation. The emitted particles are called pre-scission and post-scission particles respectively. Below the Coulomb barrier energies, the (projectiles and target) ions do not interact. Thus

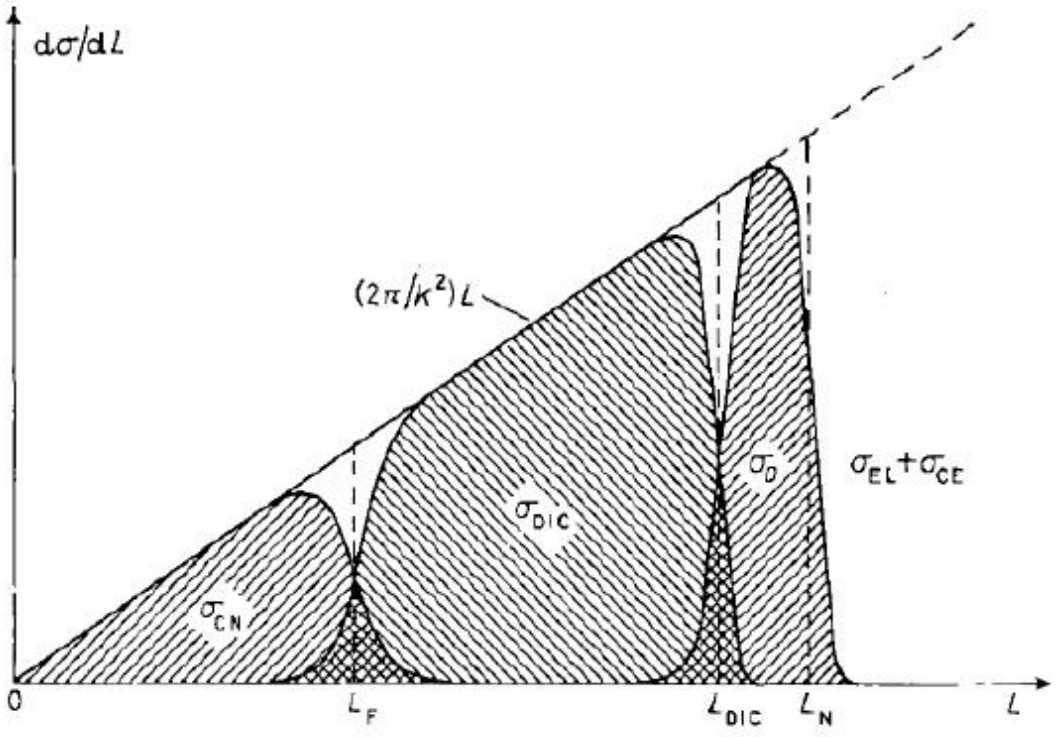

Figure 1.2: Decomposition of the total reaction cross-section into different components as a function of the orbital angular momentum parameters at which they occur.

only the Coulomb field is experienced by the interacting (projectiles and target) ions, leads to Rutherford scattering and probably Coulomb excitation. At above Coulomb barrier energies, the (projectiles and target) ions communicate via the nuclear potential. Thus other reactions like inelastic scattering, transfer reactions processes become possible. It is appropriate to discuss the interaction in terms of the impact parameter b with the interaction radius R_{int}=(R_1+R_2) where R_1 is the projectile and R_2 is the target radius.

(i) When impact parameter b is nearly equal to R_{int} (b$\sim$ R_{int}), grazing collisions take place where the direct reactions are effective.

(ii) When impact parameter b is very much smaller than R_{int} (b$\ll$ R_{int}), the projectile move toward very close to the target and thus can now also experience the strong attractive nuclear potential. Thus, the compound nuclear reactions occur in this region.

(iii) When impact parameter b is smaller than R_{int} (b$<$ R_{int}), the deep inelastic scattering occur, in which the interacting (projectile and target)ions lose a very large fraction of their energy.

Different reactions depend on the range of values of the impact parameter, the corresponding cross-sections.

According to the semi classical theory

dσ = 2πbdb and l = kb where b = l/k, db = dl/dk

$$d\sigma = 2\pi \frac{l}{k} \frac{dl}{dk} \frac{d\sigma}{dl} = \frac{2\pi}{k^2 l} = 2\pi\lambda^2 l \tag{1.5}$$

Fig.1.2 shows the total reaction cross section versus orbital angular momentum for different components [12]. According to figure,

(i) Compound nuclear reactions occur when l=l_f.

(ii) Direct reactions like quasi-elastic scattering processes and deep inelastic scattering occur when l_f $<$ l$<$$l_{DIC}$.

(iii) In case of elastic scattering and Coulomb excitation, l>l_n.

Elastic scattering is the simplest nuclear reaction between a projectile and a target that is important source of information on nuclear properties. This information has been gleaned primarily through studies of the potential of interaction (optical potential) that is found to reproduce measurements of the elastic scattering cross sections and threshold anomaly (TA)/ breakup threshold anomaly (BTA) [1].

1.2 Motivation of the thesis work

1.2.1 Study of threshold / breakup threshold anomaly

Earlier observations indicate that something unexpected was happening for heavy-ion bombarding energies in the vicinity of the top of the Coulomb barrier were provided by optical model analyses of elastic scattering measurements. The anomaly consists of a rapid and localized variation with energy E of the heavy-ion optical potential in this energy domain.

There are two main features. First, the strength of the imaginary potential W(E), at least in the surface region to which the elastic scattering of heavy ions is most sensitive, was found to increase rapidly as the energy above the top of the Coulomb barrier and then appeared to saturate at a more or less constant value. This behavior was observed to be accompanied, over the same energy range, by a rapid decrease in the strength of the attractive real potential in the same surface region, until at higher energies it assumes a constant value or a smooth, slow variation with energy E. Several aspects of heavy ion reactions have been investigated over recent decades from the analysis of elastic scattering data using different optical model codes. One of the most important features of the heavy ion elastic scattering at energies close to the Coulomb barrier is the peculiar behavior of the optical potential, known as the threshold anomaly (TA) [1, 2, 5, 13, 14, 15, 16, 17]. The real and imaginary optical

potential parameters vary strongly at beam energies below the Coulomb barrier.
In the case of threshold anomaly the real optical model potential increases as the energy decreases below the Coulomb barrier and imaginary part of optical potential decreases with the energy.The rapid decrease of the imaginary part of the optical potential below the barrier leads to a local peak in real part and this behavior can be understood using a dispersion relation between the real and the imaginary parts of the optical potential [1, 13, 18]. The dispersion relation may be obtained by using the linear segment model [19] and is given by equation 1.6. In this thesis work, the dispersion relation has been employed as a function of energy at sensitivity radius to the phenomenological optical model potentials, demarcated at every energies around the Coulomb barrier. According to the linear segment method [19], it is applied in the imaginary part of optical model potential in commandment to get the real optical model potential. For the calculation of linear segment model we can take one, two or n sets of imaginary part (according to experimental data) in order to get the real part, we used numerical calculation of equation (1.6) taking these different sets of line segment fits of imaginary optical model potential [20].

$$\Delta V\left(E\right)=\frac{P}{\pi}\int_{-\infty}^{+\infty}\frac{W\left(E'\right)}{E'-E}\,dE' \tag{1.6}$$

Also,

$$V\left(E\right)=V_o+\Delta V\left(E\right) \tag{1.7}$$

where, P is the principal value of the integral, V(E) is dynamical real potential, ΔV is dynamical polarization potential. V_o is independent of energy and W(E) is energy dependent imaginary potential.

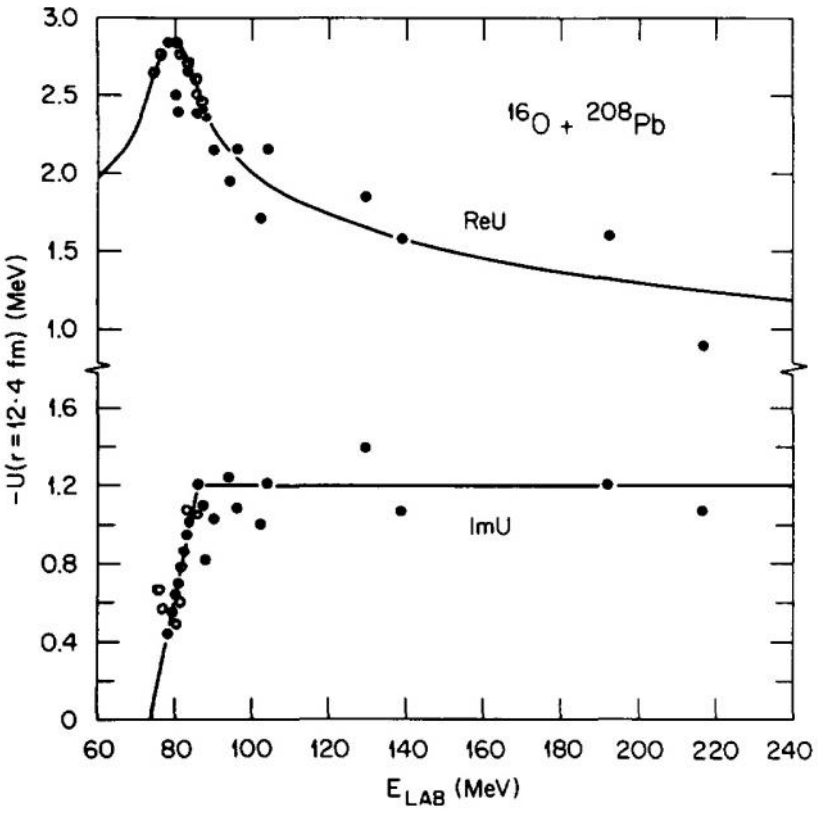

Figure 1.3: Example of Threshold anomaly for ^{16}O + ^{208}Pb [1].

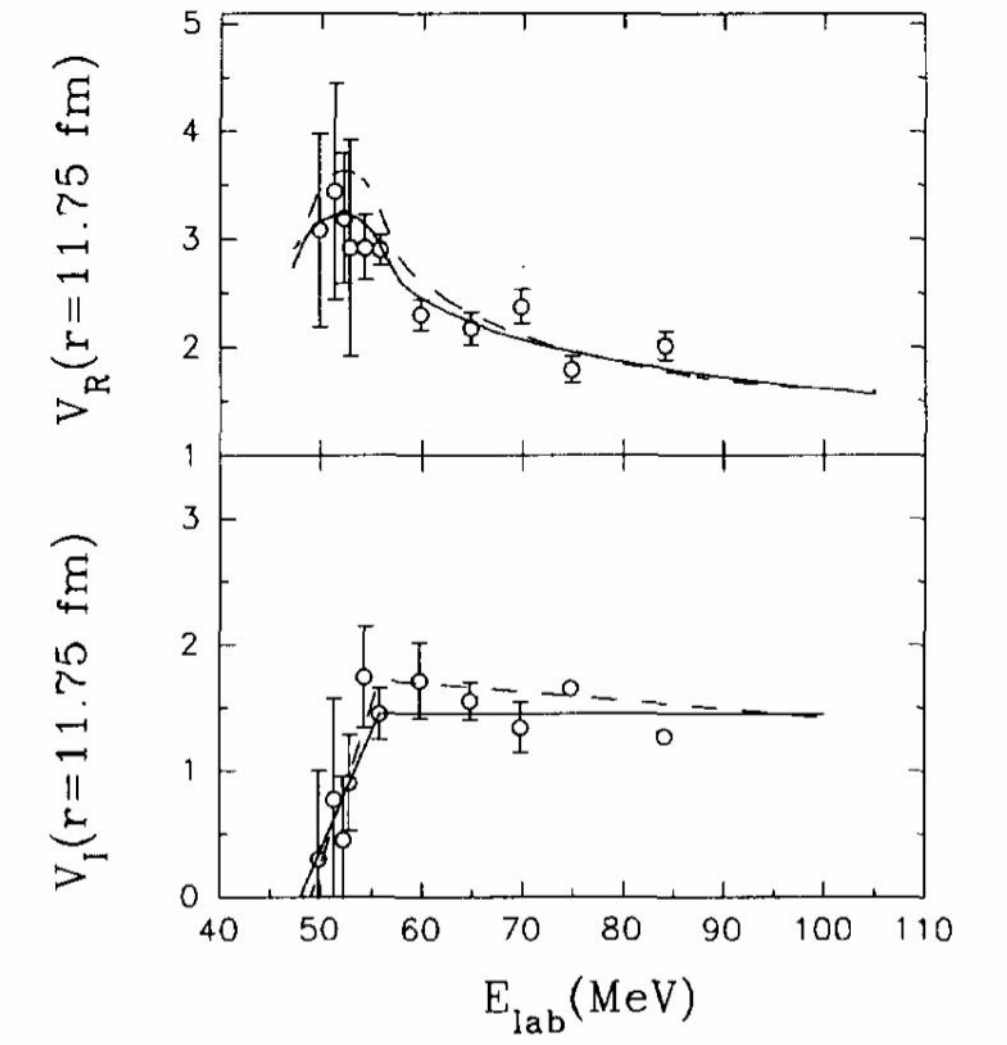

Figure 1.4: Example of Threshold anomaly for $^{11}B + ^{209}Bi$ [2].

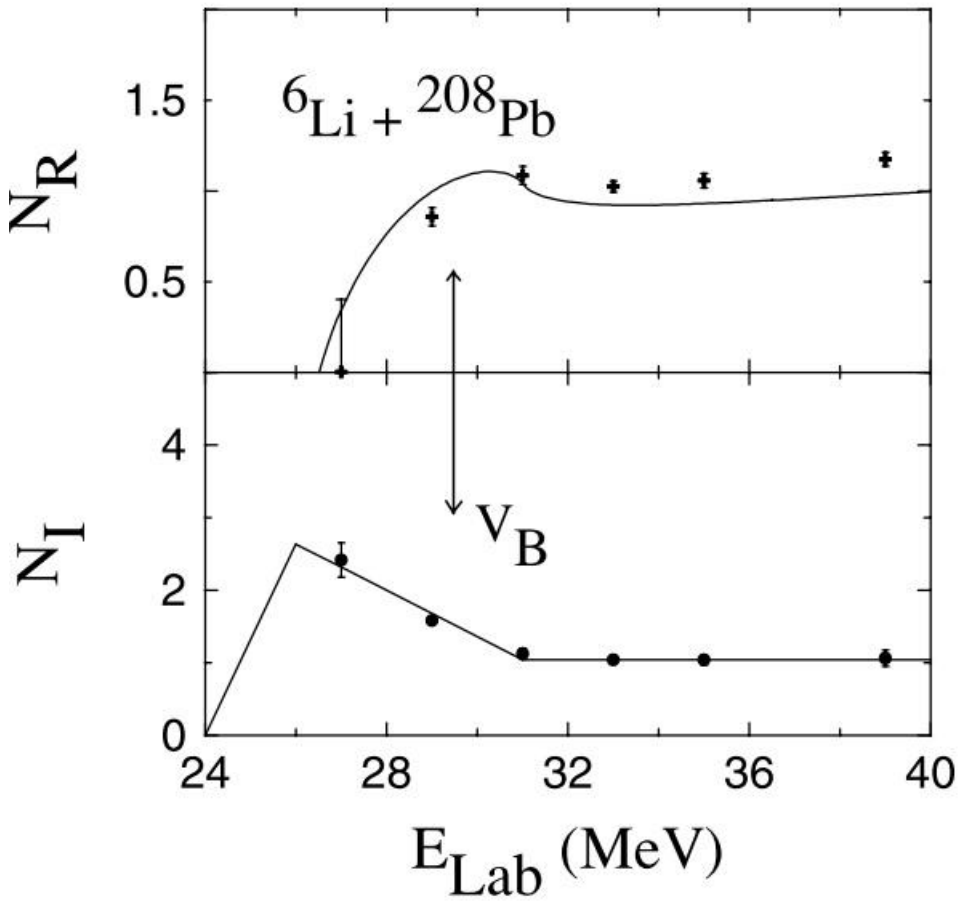

Figure 1.5: Example of breakup threshold anomaly for ^{6}Li + ^{208}Pb [3] .

Figures 1.3 and 1.4 represent the threshold anomaly for $^{16}O + ^{208}Pb$ [1] and $^{11}B + ^{209}Bi$ [2] respectively. The "threshold anomaly" is observed in many heavy-ion scattering systems. For both $^{16}O + ^{208}Pb$ [1] and $^{11}B + ^{209}Bi$ [2] systems experimental data have been consistence with the threshold anomaly.
In the case of weakly bound projectile a different type energy dependency shows around the Coulomb barrier and this behavior is totally opposite from threshold anomaly. This different type energy dependency has been known as breakup threshold anomaly (BTA) [3, 4, 5, 15, 16, 21, 22, 23, 24, 25, 26, 27]. In case of breakup threshold anomaly imaginary optical potential parameters increases and real optical potential parameters decreases because a repulsive polarization potential is produced in the pairing of breakup reactions to the elastic scattering. Figures 1.5 and 1.6 represent the breakup threshold anomaly for $^{6}Li + ^{208}Pb$ [3] and $^{6}Li + ^{64}Zn$ [4] respectively

Breakup threshold anomaly has been observed in weakly bound projectiles like ^{6}Li which has no bound exited state and the breakup threshold energy is 1.48 MeV. For $^{6}Li + ^{208}Pb$ [3] experimental data has been analyzed by the phenomenological Sao Paulo (SPP) double-folding potential. For $^{6}Li + ^{64}Zn$ [4] system, Optical model analysis of the elastic-scattering angular distributions was performed using two different model potentials (i) the double-folding real and imaginary parts of the nuclear potential, and (ii) the double-folding real potential and the phenomenological imaginary potential of the Woods-Saxon form. The results $^{6}Li + ^{208}Pb$ and $^{6}Li + ^{64}Zn$ both systems are consistence with breakup threshold anomaly.

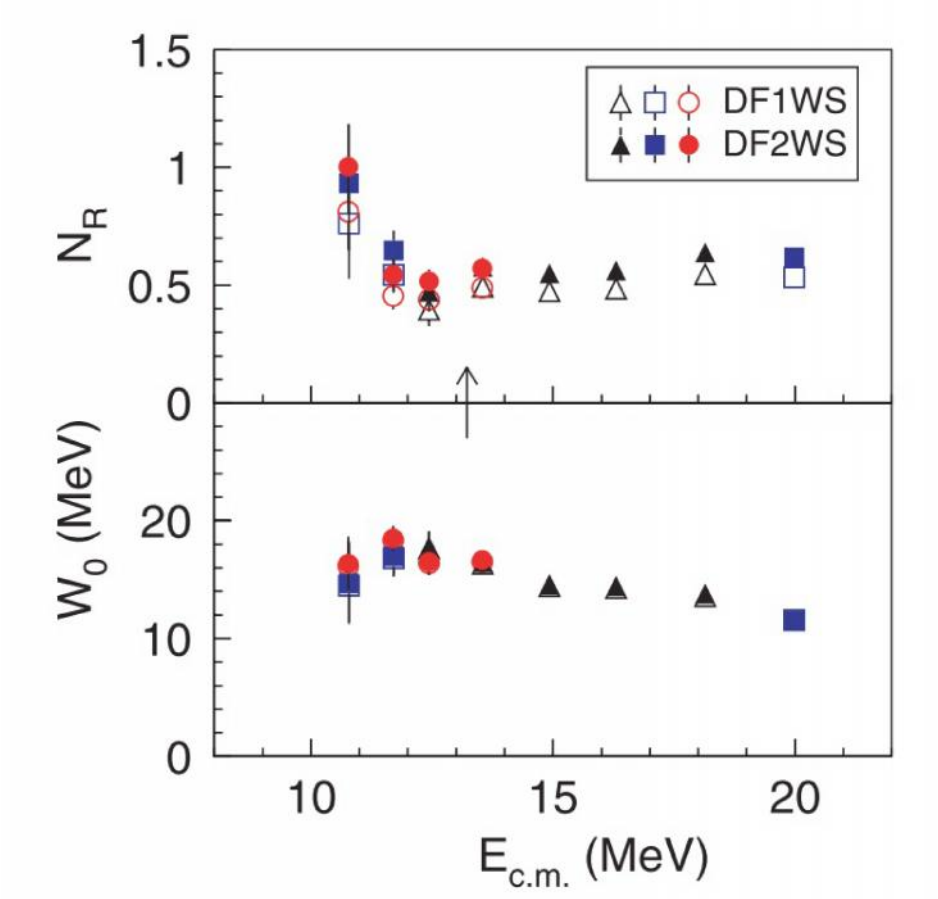

Figure 1.6: Example of breakup threshold anomaly for ^{6}Li + ^{64}Zn [4].

1.2.2 Studies of elastic, quasi elastic and transfer angular distribution involving weakly ^{6,7}Li and tightly ^{10,11}B projectiles ^{232}Th system

One of the most important techniques for prevalent information about the qualities of excited states in nuclei has been that of elastic scattering. This is due to the intervention between the amplitudes for Rutherford and nuclear scattering which, according to theory allows the phase and magnitude of the nuclear amplitude to be informed since the Coulomb amplitude is known. Maximum experimental data has been collected about the competency of excited levels from neutron, proton, and alpha-particle scattering.

However, the scattering of weakly bound projectiles, has mainly been studied at around the Coulomb barrier energies at which optical model parameters are obtained. Thus these optical model parameters have been successfully used to obtain threshold and breakup threshold anomaly. Through experimental data of elastic, quasi elastic scattering angular distribution one may obtain another important information that is known as the reaction cross section. In the elastic scattering of ^{6,7}Li on ^{80}Se target, briefly mentioned in [5], very precise angular distributions were obtained at around the Coulomb barrier energies. For this purpose, they had used eight surface-barrier detectors. An optical model analysis of the data was performed with phenomenological double-folding potential. The real and imaginary potentials were evaluated at a small separation energy, close to the strong absorption radius. The results for ^{7}Li and ^{6}Li are shown on the left and on the right panels of Fig. 1.7, respectively.

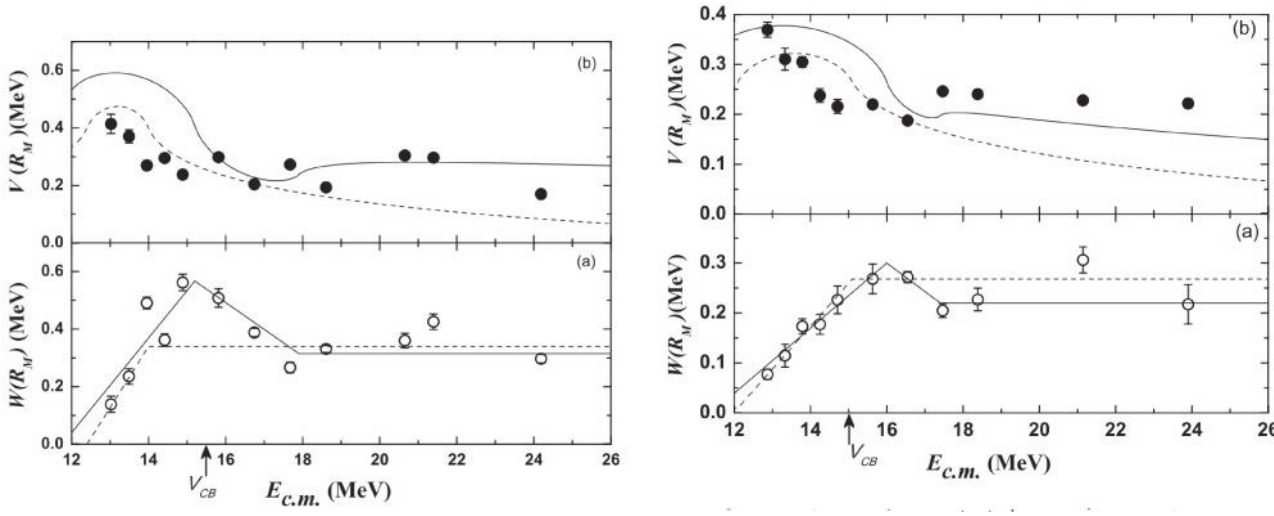

Figure 1.7: Example of the real and imaginary potentials, at the strong absorption radius, for the elastic scattering of ^{6,7}Li + ^{80}Se [5].

According to the results, we can say that these isotopes show the difference in the real and imaginary optical potential parameters. The real part of potential for ^{7}Li projectile increases while on the other hand the imaginary part of potential decreases with decrease in the energy. For ^{6}Li projectile the result is opposite to what had been observed for ^{7}Li projectile, where the imaginary part of potential increases and real part of potential decreases with the decrease in energy. Several works are available for these projectiles with different targets ^{208}Pb [16], ^{138}Ba [15]. For ^{9}Be projectile, the breakup threshold energy is 1.57 MeV and therefore, it is expected to exhibit BTA. However, recently Camacho *et al*. have carried out a detailed analysis of the energy dependence of the optical potentials for the ^{9}Be + ^{208}Pb,^{209}Bi systems [28]. It is reported that the imaginary potential indicates the presence of usual TA in these reactions, similar to that observed in tightly bound systems, but the direct reaction imaginary potential shows a BTA behavior. There are very limited elastic scattering data for ^{10}B and ^{11}B projectiles with heavy targets ^{209}Bi and the result of ^{11}B + ^{209}Bi system is consistence with threshold anomaly [2, 17]. For this system experimental data has been analysed by using a microscopic double-folded real potential and a phenomenological volume Woods-Saxon imaginary potential at the various energies [2].

To the best of our knowledge there have been no measurements reported for ^{10,11}B projectiles on heavy mass target ^{232}Th. The methodical analysis of the energy dependence of real and imaginary optical potential parameters for the ^{10,11}B + ^{232}Th reactions are important to establish the presence of TA/BTA in these reactions. The use of the heavy target in the investigation of TA/BTA has the advantage, as the effect is expected to be more pronounced due to large Coulomb barrier. This motivated us to undertake the study of TA/BTA on the ^{6,7}Li + ^{232}Th and ^{10,11}B + ^{232}Th systems.

1.3 Objective of the thesis

The present work has been carried out with the following objectives.

(i) To experimentally measure the elastic scattering angular distribution around the Coulomb barrier energies for the weakly bound projectiles ^{6,7}Li on the heavy mass target ^{232}Th.

(ii) To obtain the quasi elastic scattering and transfer angular distribution around the Coulomb barrier energies for the tightly bound projectiles ^{10,11}B on heavy mass target ^{232}Th.

(iii)The theoretical analysis have been carried out with ECIS (Equations Couplpees en Itperations Spequentielles) by using the Woods Saxon and double folding Sao Paulo potential. These calculations were undertaken to study the threshold and breakup threshold anomaly in weakly (^{6,7}Li) and tightly (^{10,11}B) bound projectile on the heavy mass target ^{232}Th below and around the Coulomb barrier energies.

The elastic scattering, quasi elastic scattering and transfer angular distribution measurements have been carried out at BARC-TIFR Pelletron facility, in Mumbai India. In ^{6,7}Li + ^{232}Th systems measurements, threshold anomaly has been observed in ^{7}Li + ^{232}Th system and breakup threshold anomaly has been observed in ^{6}Li + ^{232}. In ^{10,11}B + ^{232}Th measurements, threshold anomaly have been observed for both systems.

1.4 Brief literature survey

During the last many decade, experiments have been performed in order to study the threshold and breakup threshold anomaly by elastic and quasi elastic scattering angular distributions with light, medium and heavy mass targets. In the case of ^{7}Li projectile on different targets such as, ^{59}Co [14], ^{138}Ba [15], ^{208}Pb [16], ^{232}Th [29] and ^{80}Se [5] the threshold anomaly was identified. In case of some other heavy ions systems also

threshold anomaly have been observed ^{12}C [30],^{16}O [1, 13, 31, 32, 33]. One of the important feature from the observation of threshold and breakup threshold anomaly is that a strong energy dependence optical potential parameters selected at the energies around the Coulomb barrier through the analysis of elastic scattering scattering angular distributions.

The rapid variation of the imaginary part of the optical potential near the barrier leads to a corresponding strong energy dependence of the real part "threshold anomaly" [2]. In case of weakly bound projectile ^{6}Li results of TA/BTA are available on several targets like, (^{27}Al, ^{64}Ni, ^{64}Zn, ^{90}Zr, ^{138}Ba, ^{144}Sm, ^{208}Pb, ^{209}Bi, ^{116,112}Sn, ^{232}Th and ^{80}Se) [4, 5, 24, 25, 22, 23, 15, 16, 26, 27, 29]. In case of tightly bound projectile ^{10,11}B, threshold anomaly have been observed and very limited work is available [2, 17, 34]. In case ^{9}Be projectile BTA has been observed ^{208}Pb, ^{209}Bi systems [28].

1.5 Structure of the thesis

In this thesis, the research work carried out and compiled has been published in peer reviewed journals [29, 34, 35]. An overview of this thesis content has been grouped into five chapters as follows:

The **Chapter 1** gives a general introduction of the thesis subject. It begins with basic nuclear reaction mechanism when projectile and target come close to each other. Further this chapter broadly describes the study involving ^{6,7}Li and ^{10,11}B on ^{232} Th target.

In the beginning of **Chapter 2** a brief introduction to the BARC-TIFR Pelletron accelerator facility at Mumbai is presented. Further this chapter describes the performance characteristics of various radiation detectors used to carry out the experiments as discussed in the present thesis work. The chapter also discusses the particle identification technique, interaction of charge particles with matter. In this **chapter** short description of the models used have been given, and how the model which we have

used is of prime importance for our study has been discussed. In order to check the consistency of the results obtained, we have analyzed our data using two different kinds of potential so as to study the reaction mechanism. The two different kind of potential have also been mentioned in this chapter.

The **Chapter 3** is devoted essentially to the measurement of elastic scattering angular distribution and dispersion relation of ^{6,7}Li + ^{232}Th systems. Here also the experimental procedure and analysis work, have been briefly discussed along with calculated total reaction cross sections of ^{6,7}Li + ^{232}Th systems. Finally present result and conclusions have been discussed.

In **Chapter 4** the measurement of quasi elastic scattering, transfer angular distribution and dispersion relation of ^{10,11}B + ^{232}Th systems, have been discussed. In this chapter, the experimental procedure and analysis work have been discussed along with calculated total reaction and transfer cross sections of ^{10,11}B + ^{232}Th systems. At the end of the chapter, the results obtained for ^{10,11}B + ^{232}Th systems have been discussed and conclusions were drawn therefrom.

The **Chapter 5** gives a brief summary of the research work carried out in this thesis along with the final conclusions and future outlook.